Journal of Supramolecular Structure 11:401–427 (1979)
Tumor Cell Surfaces and Malignancy 281–307

Fibronectin and Proteoglycans as Determinants of Cell-Substratum Adhesion

Lloyd A. Culp, Ben A. Murray, and Barrett J. Rollins

Department of Microbiology, Case Western Reserve University, Cleveland, Ohio 44106

When normal or SV40-transformed Balb/c 3T3 cells are treated with the Ca^{++}-specific chelator EGTA, they round up and pull away from their footpad adhesion sites to the serum-coated tissue culture substrate, as shown by scanning electron microscope studies. Elastic membranous retraction fibers break upon culture agitation, leaving adhesion sites as substrate-attached material (SAM) (Cells leave "footprints" of substrate adhesion sites during movement by a very similar process.) SAM contains 1–2% of the cell's total protein and phospholipid content and 5–10% of its glucosamine-radiolabeled polysaccharide, most of which is glycosaminoglycan (GAG). By one- and two-dimensional sodium dodecyl sulfate-polyacrylamide gel electrophoresis, there is considerable enrichment in SAM for specific GAGs; for the glycoprotein fibronectin; and for the cytoskeletal proteins actin, myosin, and the subunit protein of the 10 nm-diameter filaments. Fibrillar fibronectin of cellular origin and substratum-bound fibronectin of serum origin (cold-insoluble globulin, CIg) have been visualized by immunofluorescence microscopy. The GAG composition in SAM has been examined under different cellular growth and attachment conditions. Heparan sulfate content correlates with glycopeptide content (derived from glycoprotein). Newly attaching cells deposit SAM with principally heparan sulfate and fibronectin and little of the other GAGs. Hyaluronate and chrondroitin proteoglycans are *coordinately* deposited in SAM as cells begin spreading and movement over the substrate. Cells attaching to serum-coated or CIg-coated substrates deposited SAM with identical compositions. The proteoglycan nature of the GAGs in SAM has been examined, as well as the ability of proteoglycans to form two classes of reversibly dissociable "supramolecular complexes" – one class with heparan sulfate and glycopeptide-containing material and the second with hyaluronate-chondroitin complexes. Enzymatic digestion of "intact" SAM with trypsin or testicular hyaluronidase indicates that (1) only a small portion of long-term radiolabeled fibronectin and cytoskeletal protein is bound to the substrate via hyaluronate or chondroitin classes of GAG; (2) most of the fibronectin, cytoskeletal protein and heparan

Abbreviations: EGTA, ethylenebis (oxyethylenenitrilo) tetra acetic acid; SAM, substrate-attached material; SDS, sodium dodecyl sulfate; PAGE, polyacrylamide gel electrophoresis; BSA, bovine serum albumin; GAG, glycosaminoglycan; GAP, glycosaminoglycan-associated protein; CIg, cold-insoluble globulin; TPCK, L-1-tosylamide-2-phenylethylchloromethyl ketone; PMSF, phenylmethylsulfonyl fluoride; PBS, phosphate-buffered saline.

Received April 9, 1979; accepted July 6, 1979.

0091-7419/79/1103-0401$04.70

sulfate coordinately resist solubilization; and (3) newly synthesized fibronectin, which is metabolically labile in SAM, is linked to SAM by hyaluronate- and/or chondroitin-dependent binding. All of our studies indicate that heparan sulfate is a direct mediator of adhesion of cells to the substrate, possibly by binding to both cell-surface fibronectin and substrate-bound CIg in the serum coating; hyaluronate-chondroitin complexes in SAM appear to be most important in motility of cells by binding and labilizing fibronectin at the periphery of footpad adhesions, with subsequent cytoskeletal disorganization.

Key words: **fibronectin, glycosaminoglycans, proteoglycans, adhesion, substrate-attached material cytoskeleton, immunofluorescence, heparan sulfate**

Adhesive interactions between cells and between cells and noncellular matrix materials appear to be involved in a number of interesting and important biological processes, including normal and abnormal morphogenesis and malignant invasion. Many workers have studied the biological properties of these adhesive interactions and have demonstrated both quantitative and qualitative differences in adhesion that may be biologically important, but the underlying molecular mechanisms have been difficult to unravel [1].

Recently, fibronectin, a large protein found on the surface of many vertebrate cells [2, 3] and in vertebrate plasma, where it is known as cold-insoluble globulin (CIg) [3], has been shown to be involved in the normal adhesion of some avian and mammalian cell types to extracellular substrata [1]. For many cell types, fibronectin must be adsorbed to the substratum for normal cell attachment and spreading to occur [4], and addition of exogenous fibronectin causes many poorly adherent transformed cell lines, which are depleted of surface fibronectin, to spread out and adhere more tightly to the substratum [3]. The mechanism(s) by which fibronectin brings about these effects is unknown, but the known affinity of fibronectin for fibrous matrix materials such as collagens [5, 6] and heparin [7] raises the possibility that fibronectin may directly mediate in some fashion an adhesive interaction involving cells, fibrillar components, and fibronectin (cellular and/or substratum-bound). This possibility is strengthened by the demonstration that anti-whole-cell antibodies or concanavalin A, when bound to culture dishes, can mediate BHK cell attachment and spreading, which is morphologically and kinetically similar to that seen when dish-bound fibronectin is employed [8].

Clearly, it would be easier to study such molecular interactions in adhesion if the adhesive cell surface sites could be at least partially purified away from the rest of the cell. Such a preparation can be generated from a variety of cell types by treatment with the calcium-specific chelator EGTA [9]. The cells round up and retract away from their substrate adhesion sites; the retraction fibers connecting the cells to the adherent material eventually break, leaving the adhesion sites and associated material still firmly bound to the dish [10]. In the past few years we and our colleagues have examined the cellular origins and biochemical composition of this substrate-attached material (SAM) in some detail [1, 9–21]. More recently, we have begun experiments to examine the structural and functional interrelationships between the various components of SAM [15; Rollins and Culp, in preparation]. Although our results are not yet conclusive, they suggest that fibronectin in SAM is specifically associated with certain classes of glycosaminoglycans and proteoglycans. These interactions, then, may be part of the molecular mechanism of cell-substratum adhesion.

GROSS COMPOSITION OF SUBSTRATE-ATTACHED MATERIAL

Initial studies in our laboratory showed that SAM contains 1–2% of the cell's total protein content (as detected by incorporation of radiolabeled leucine) and 5–10% of the cell's polysaccharide (as detected by incorporation of radiolabeled glucosamine) [21]. There is little or no detectable nucleic acid, showing that SAM does not simply consist of a small number of cells that are resistant to detachment. Most of the polysaccharide represents glycosaminoglycans (GAGs) [12, 16], which drew our attention to these long-chain polysaccharides as possible mediators of adhesion. More recently Cathcart and Culp [14] have shown that SAM also contains 1–2% of the cell's phospholipid. These results, together with scanning electron microscopic studies discussed below, suggested that SAM represents discrete regions of the cell surface specialized for adhesion. Further work in our laboratory has been designed to test this hypothesis and to dissect further the structure and function of the components of SAM.

SAM REPRESENTS CELL-SUBSTRATUM ADHESION SITES

If biochemical studies of SAM are to have any relevance to cell-substratum adhesion, it is essential to show that SAM does not represent material that is secreted by the cells into the medium during growth or EGTA-mediated detachment and that then binds secondarily to the substratum. Contamination of SAM by whole cells is routinely less than 0.01%. Autoradiographic experiments with SAM metabolically labeled with ^{3}H-leucine or ^{3}H-glucosamine show that most of the incorporated label is found specifically located in areas to which cells were formerly attached and not in areas of the substratum that were free of cells [17]. Fibronectin shows a similarly restricted distribution when visualized by indirect immunofluorescence (see below). Furthermore, deposition of radiolabeled SAM onto the substratum ceases when the cells have completely covered the substratum, although the amount of radiolabeled macromolecular material shed into the medium continues to increase [19]. At least some of this material should have access to the substratum, since antibody is able to penetrate under the cells (see below).

There is considerable evidence that SAM represents the areas by which the cells are tightly bound to the tissue culture substratum, probably through the mediation of a tightly adsorbed layer of serum proteins. Micromanipulation experiments indicate that many cell types adhere to the substratum at multiple focal adhesive plaques [22]. SAM is indeed tightly adherent to the dish; the material is largely resistant to extraction with a wide variety of nonionic detergents, chaotropic agents, and salts [Cathcart and Culp, in preparation]. Of all the treatments tested, only extraction with 0.2% sodium dodecyl sulfate quantitatively solubilizes both protein and polysaccharide. Extraction with 0.5% sodium deoxychloate, 5 M urea, or 0.5% nonionic detergent (Triton X-100, Nonidet P-40, or Tween 40) solubilized 40% or less of either material. Sodium dodecyl sulfate-polyacrylamide gel electrophoresis (SDS-PAGE) patterns of solubilized and resistant material after these treatments were generally very similar, one exception being that part of the actin in SAM could be selectively extracted by nonionic detergent or by ATP plus KCl [Cathcart and Culp, in preparation]. Thus, the great majority of proteins and polysaccharides in SAM are *coordinately* released or retained, arguing that these materials are indeed structurally associated in SAM. High-resolution autoradiography [17] and immunofluorescent staining of fibronectin (see below) reveal that SAM components are distributed in localized pools under the cell. Material of similar morphology can be visualized by scanning electron micro-

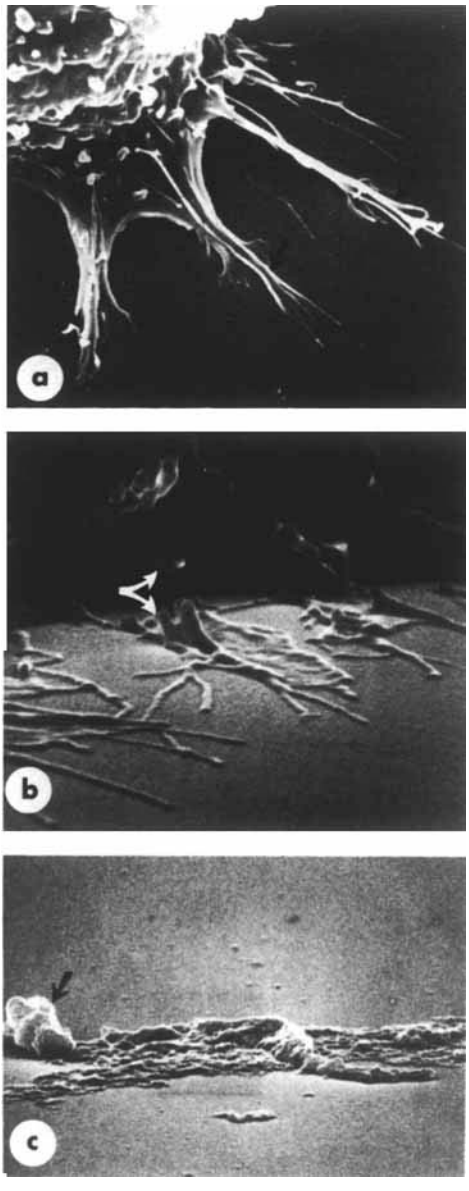

Fig. 1. Cellular origin of substrate-attached material. Swiss 3T3 cells were detached by EGTA treatment after growth to confluence and then allowed to reattach to fresh glass substrate in medium containing 10% serum. Specimens were processed for scanning electron microscopic observation by fixation in buffered glutaraldehyde, dehydration with graded alcohols and freon, and critical-point drying. Samples were sputter-coated with gold-palladium before SEM analysis. (a) A cell 2 h after attachment, showing well-developed footpads at the arrows (original magnification, × 6,500; 20° tilt); (b) a cell detaching after 10 min of treatment in 0.5 mM EGTA in PBS with gentle shaking, showing shearing of the labile retraction fiber (at the arrows) that connects the cell body to the footpad (original magnification, × 13,500; 80° tilt); (c) morphology of SAM after removal of cells that had been grown for 24 h, showing the remnant of the retraction fiber at the arrow (original magnification, × 13,500; 80° tilt). (Reprinted from Culp et al [20], with permission of the publisher.)

scopy of SAM (Fig. 1) [10, 20] and of material left behind after mechanical removal of cells [23–26]. When cells are examined microscopically during the detachment process, they are seen to round up and retract away from this firmly bound material (Fig. 1) [10, 20]. Finally, SAM differs in protein [11, 27], phospholipid [14], and polysaccharide [12] composition from whole cell or enriched surface membrane preparations, suggesting that it represents a specialized region of the cell surface. For example, SAM, whole cell preparations, and enriched membrane fractions prepared by two different methods all have the same classes of phospholipids present, but SAM is enriched for phosphatidylserine and has a higher ratio of phosphatidylethanolamine to phosphatidylcholine than do other preparations [14].

Proteins of SAM

The protein composition of SAM has been investigated by sodium dodecyl sulfate-polyacrylamide gel electrophoresis (SDS-PAGE) of the SDS-extracted radiolabeled material (Fig. 2). A number of species are enriched with respect to solubilized whole membranes. In particular, fibronectin (C_0), myosin (C_a), and actin (C_2) can be identified. By analogy with other systems [30–33], C_1 represents the subunit protein of one or more types of 10 nm "intermediate" filaments. SAM contains, at most, trace amounts of collagen [13], so collagen does not appear to be involved in cell-substratum adhesion in this system.

To resolve further the biochemical complexity of the proteins in SAM and to assist in further identifying the unknown components, we turned to the high-resolution two-dimensional electrophoresis system described by O'Farrell [34]. Proteins are isoelectrically focused in a cylindrical gel in the first dimension, followed by sizing analysis on a slab SDS-PAGE gel in the second dimension.

When substrate-attached proteins were analyzed on two-dimensional gels, a minor radioactive cellular protein, identified as "α" in Figure 3, co-electrophoresed with porcine skeletal α-actinin [28]. The concentrations of this α-actinin-like protein in SAM were very low compared to the amounts of actin and myosin. A minor band in the SAM of these cells, which migrates more slowly than the C_b band, has recently been shown to bind monospecific antibody to α-actinin [J. Schollmeyer, personal communication]. The presence of α-actinin in substrate adhesion sites is of considerable interest, since this protein may be the internal membrane attachment site for actin-containing microfilaments in gut epithelial microvilli [29]. Also, the immunofluorescent distribution of α-actinin in spreading rat embryo cells exhibits a condensed focal pattern similar to the pattern observed with anti-actin [30], and some of these condensed foci may be cell-substrate adhesion sites. Other evidence will be required to determine if this protein acts as the internal membrane binding component for the actin-containing microfilaments in these adhesion sites; however, the very small quantity of this protein in SAM may argue against a major anchorage role for this protein.

The C_b band in Figure 2 is resolved into two components on two-dimensional gels – the major component, C_{b1}, and the minor component, C_{b2}, in Figure 3. Neither of these components appears to be glycosylated, since precursor radioactive glucosamine cannot be incorporated into the C_b bands [11]. Fibronectin (C_0) displays considerable microheterogeneity in the isoelectric focusing direction, some of which may be derived from the fact that it is a sialylated glycoprotein [27]. This microheterogeneity is probably not due to a monomer-dimer equilibrium via disulfide crosslinkage [35], since isoelectric focusing was performed with samples in 5% mercaptoethanol.

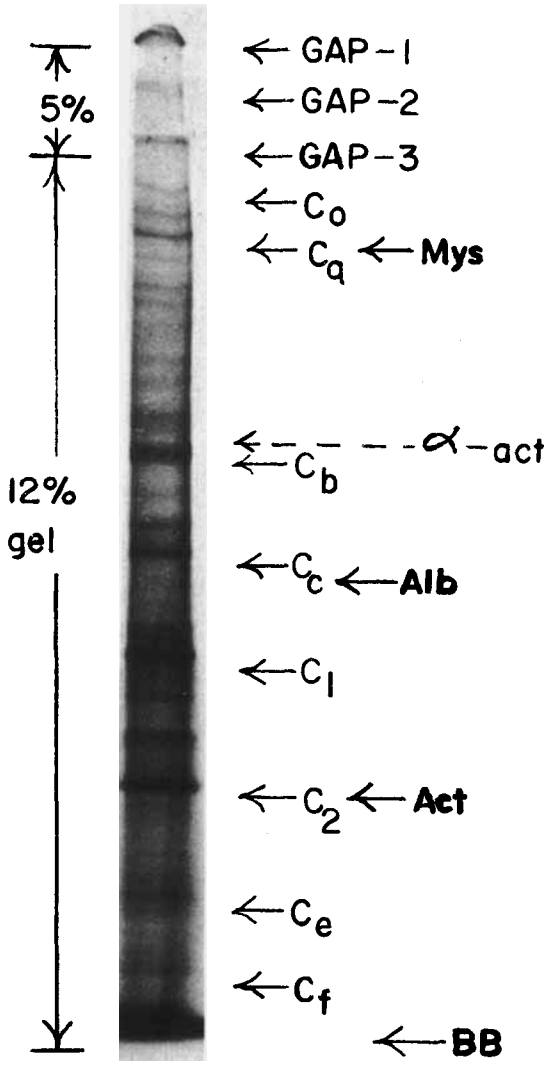

Fig. 2. Slab SDS-PAGE analysis of leucine-radiolabeled SVT2 substrate-attached material. As described previously [11], ^{14}C-leucine-radiolabeled SVT2 SAM was prepared after growth of cells for 48 h in radioactive medium, and the SAM was harvested by SDS extraction after EGTA-mediated detachment of cells. 20,000 cpm of SAM in sample buffer were electrophoresed in a 12% ORTEC slab gel at 40 mA/gel. The gel was then dried and autoradiographed for 8 weeks. Marker proteins of rabbit skeletal muscle myosin (Mys), rabbit skeletal muscle actin (Act), bovine serum albumin (Alb), and porcine skeletal muscle α-actinin (α-act) were electrophoresed on the same gel and detected by staining with Coomassie blue. The nomenclature for cellular proteins (C) in SAM has been described previously [11, 20, 21], and the following components have been identified: GAP, glycosaminoglycan-associated protein; C_o, fibronectin; C_a, myosin; C_2, actin.

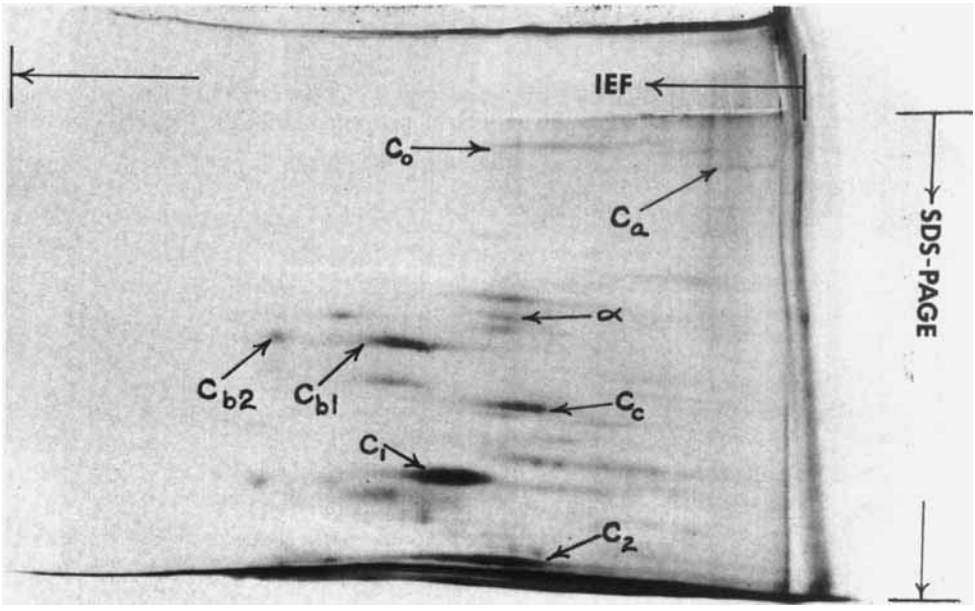

Fig. 3. Two-dimensional electrophoresis of the larger proteins in SAM. Isoelectric focusing was performed in 2 mm diameter (12 cm length) cylindrical gels as described by O'Farrell [34] using a mixture of 1.6% pH 5–7 ampholines and 0.4% pH 3–10 ampholines. These gels were frozen at −20°C until they were used for SDS-PAGE. Slab SDS-PAGE gels for the second dimension were poured in the following order: a 12% or 20% ORTEC separating gel as described previously [11], depending on the size range of proteins being analyzed; then a 2 cm length 5% ORTEC stacking gel; finally a 0.5 cm length 2% agarose gel (containing 0.075 M Tris sulfate, pH 8.4) into which was embedded the isoelectric-focused cylindrical gel. A thin layer of sample buffer was applied at the surface of the agarose gel. Electrophoresis was performed as described by O'Farrell for nonequilibrated samples at 40 mA/gel. After electrophoresis, the slab gels were dried and autoradiographed for 1–4 months. 25,000 cpm of ^{14}C-leucine-radiolabeled SVT2 SAM was isoelectrically focused (IEF) in a cylindrical gel in the first dimension. Then this gel was mounted in an agarose overlay and electrophoresed into an SDS-PAGE gel (12% ORTEC gel) as the second dimension. Basic proteins are distributed on the right side and acidic proteins on the left side of the gel. Two micrograms each of carrier rabbit skeletal muscle actin and porcine skeletal muscle α-actinin were also present in the sample and were detected by Coomassie staining – the former co-electrophoresed with radioactive component C_2 and the latter with the radioactive spot marked α. The gel was dried, and radioactive components were detected by autoradiography as shown here.

The prominent C_1 protein (mol wt 55,000), which is completely lacking in tryptophan residues and which has been shown not to be tubulin [11], migrates in these O'Farrell gels identically to the "52K" protein identified by Brown et al [31] as the subunit protein of the 10 nm-diameter, non-actin containing filaments of fibroblasts. This protein, as well as actin (C_2), is observed in SAM in similar relative concentrations from both normal and virus-transformed cells under many different growth conditions (C_1:C_2 = 0.5–0.6), suggesting that both classes of filaments are tightly associated in the substrate adhesion site of cells in a well-defined molar ratio [1, 11, 20, 21]. However, the immature adhesion sites of newly attaching, EGTA-subcultured 3T3 or SVT2 cells contain much higher levels of C_1 relative to actin or myosin (C_1:C_2 = 1.5–2.0) [11, 20, 21]. This suggests that these

filaments play an important role in reorganization of cell surface material at these adhesion sites.

Previous evidence [11, 20, 21] has demonstrated that the C_2 band is actin. When SAM preparations are electrophoresed on O'Farrell gels using 20% slab SDS-PAGE gels to improve the resolution of low molecular weight proteins, the actin band (C_2) can be resolved into two equivalent pools (Fig. 4) with different isoelectric points corresponding to the beta and gamma forms of actin observed in non-muscle cells [36, 37]. The relative amounts of the beta and gamma forms of actin were similar in SAM and whole cell extracts. It thus appears that the EGTA-resistant, adhesion-site-bound actin is not an enrichment of either class of actin and reflects the actin composition of the whole cell.

Fibronectin in SAM

Since fibronectin has been implicated in cell-substratum adhesion [3, 4], we decided to investigate the topographic distribution of this protein in SAM. Taking advantage of the immunological cross-reactivity between fibronectins of different species [38] and the easy purification of plasma fibronectin by affinity chromatography on immobilized gelatin [5, 6], we prepared, purified, and characterized monospecific goat and rabbit antibodies against human plasma fibronectin (cold-insoluble globulin; CIg) [Murray and Culp, in preparation]. The specificity of the antibodies was verified by double diffusion analysis (Ouchterlony) and crossed-immunoelectrophoresis [39]. With the immunoperoxidase-staining technique for SDS-PAGE of Olden and Yamada [40], these antibodies specifically stain a band in SAM that comigrates with authentic fibronectin (data not shown).

We first used indirect immunofluorescence analysis of formaldehyde-fixed cultures to examine fibronectin distribution before the cells were removed. The results were similar to the patterns observed by others in other cell types [3, 41, 42] (Fig. 5). Cell-associated fibronectin-specific fluorescence was visible as a pattern of supracellular fibers; the pattern grew much more extensive and more intricate as the cultures grew denser. In the sparser cultures fibrillar fluorescence often coincided with the boundary between two cells, but

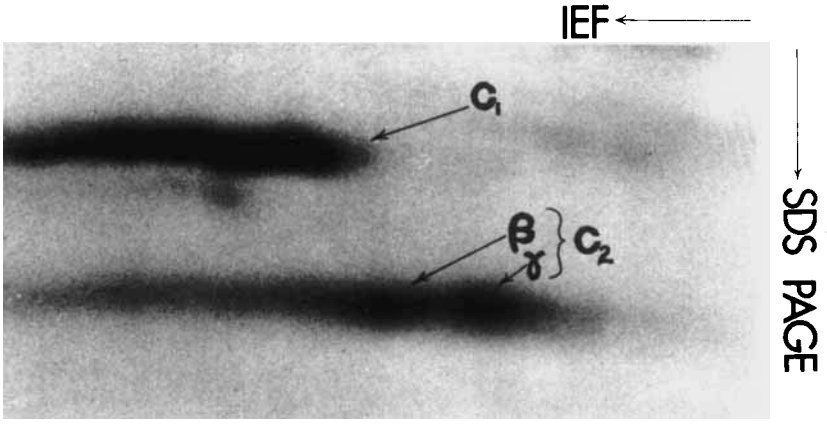

Fig. 4. Two-dimensional electrophoresis of the smaller proteins in SAM. ^{14}C-leucine-radiolabeled SVT2 SAM was electrophoresed as described in Figure 3, except a 20% ORTEC slab SDS-PAGE gel was used to improve the resolution of smaller proteins. Only a portion of the autoradiogram is shown. Rabbit skeletal muscle actin (2 μg added as carrier) co-electrophoresed with the C_2 radioactive component in SAM, which has previously been shown to be actin by a number of criteria [11, 21].

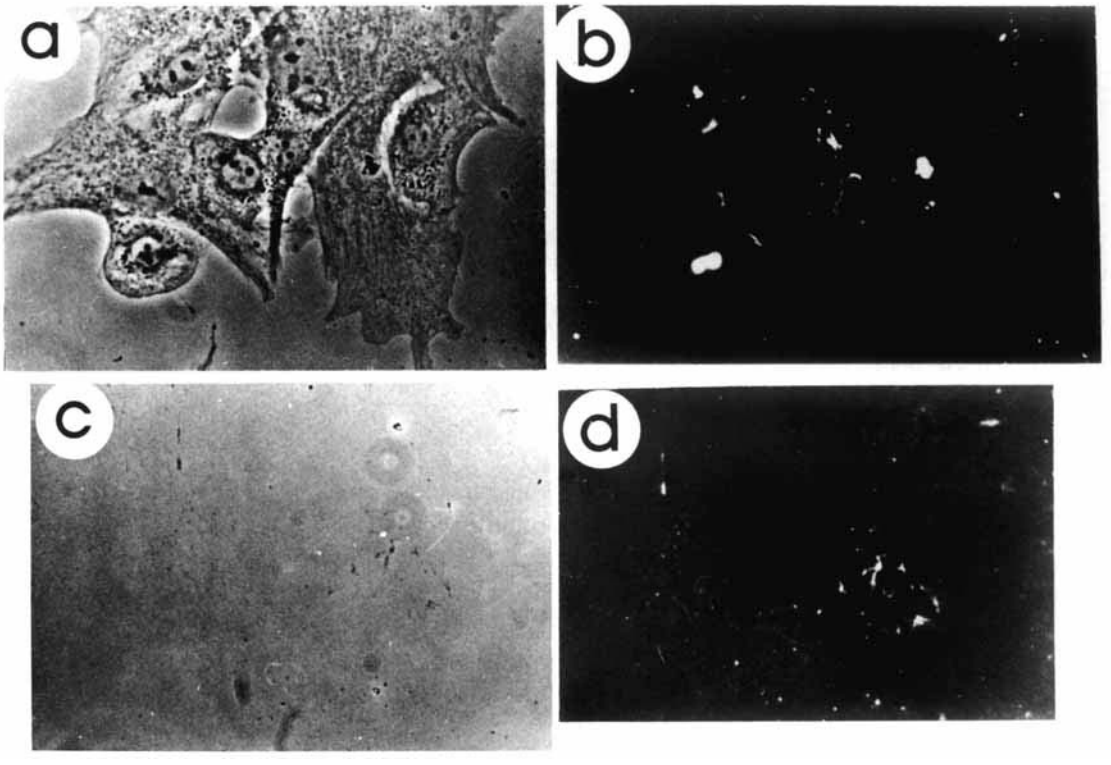

Fig. 5. Immunofluorescence analysis of Balb/c 3T3 cells and SAM. Balb/c 3T3 cells were grown on 11 × 22 cm glass coverslips as described previously [18]. At 24 h after seeding, the cells were washed three times with phosphate-buffered saline containing 1 mM each $CaCl_2$ and $MgCl_2$ and fixed for 20 min in the same buffer containing 3.7% formaldehyde. After three 5-min washes in buffer lacking formaldehyde, cells were stained for 30 min at room temperature with 4 μg/ml affinity-purified rabbit antibody directed against purified human plasma fibronectin [Murray and Culp, in preparation]. After three more washes, the coverslips were further stained with fluorescein-labeled goat antibody to rabbit immunoglobulin (Miles Laboratories, 1/64 dilution), washed, and mounted in a barbital-buffered saline solution at pH 9. For SAM preparations, cells were released from coverslips by treatment with 0.5 mM EGTA in buffer lacking divalent cations [9] followed by gentle pipetting. The coverslips were then washed and fixed (using buffer lacking divalent cations) and processed as above. Samples were examined on a Leitz Ortholux microscope equipped with phase-contrast optics and epifluorescence illumination at an original magnification of 400 ×. (a) 3T3 cells visualized by phase-contrast optics; (b) fluorescence image of the same field; (c) 3T3 SAM visualized by phase-contrast optics; (d) fluorescence image of the same field.

this correspondence was lost as the cultures grew denser. By differential focusing we could also see fluorescent fibers *underneath* the cells, suggesting that the antibody was able to penetrate between the cell and substratum; this has not been observed in all other systems [41]. This staining probably did not arise by penetration of the antibodies *through* the cell, since diffuse intracellular staining was seen only in preparations in which the integrity of the membrane had been impaired by extraction with 0.5% Triton X-100 for 5 min. The fibrillar staining was also seen with antibodies that had been absorbed with insolubilized bovine CIg, so this presumably represents fibronectin synthesized by the cells. In contrast, a continuous layer of fluorescence was visualized bound to the substratum; this staining

was abolished by the above absorption, and so it probably represents bovine CIg adsorbed to the substratum from the calf serum in the tissue culture medium. In sparse cultures, this substratum-bound fluorescence frequently was reduced or absent directly beneath and around cells and in "tracks" leading up to cells; these tracks resembled in their appearance the "phagokinetic tracks" seen by Albrecht-Buehler [43]. We do not yet know whether this decreased fluorescence is a result of the loss of substrate-bound CIg or of the masking of CIg antigenic determinants by some other material.

We found many similar features when we examined SAM by immunofluorescence (Fig. 5). There was considerable fibrillar and punctate fluorescence localized to areas of the approximate size and shape of single cells or small groups of cells. The continuous substratum fluorescence with dark "tracks" was also seen. As with the cell cultures, only the fibrillar and punctate fluorescence was stained with antibodies previously adsorbed with bovine CIg to prevent reactivity of the antibody with substratum-adsorbed serum proteins. This does not rule out the possibility that *some* of the fibrillar and punctate fluorescence may represent bovine CIg absorbed from the medium. It is interesting that the amount of fibronectin-specific fluorescence of any kind (continuous, fibrillar, or punctate) decreases drastically in SAM generated from very dense cultures grown on glass coverslips; this decrease is *not* observed on plastic coverslips (data not shown). A similar finding was briefly noted by Mautner and Hynes [41] for NIL cells. This observation is being further investigated.

Serum Components in SAM

Material synthesized by cells in SAM can be detected by incorporation of appropriately radiolabeled precursors. In addition, SAM also contains adsorbed serum proteins. At least twelve such components can be detected by SDS-PAGE analysis [11; Haas and Culp, in preparation], including bovine serum albumin (BSA). However, BSA alone will not support normal cell attachment and spreading when adsorbed to a substratum. Grinnell and others have shown that purified plasma fibronectin (CIg), when adsorbed to the substratum, will mediate normal attachment and spreading of BHK cells [4]; we have confirmed this result for Balb/c 3T3 and SVT2 cells [Murray, Haas and Culp, in preparation). It has been reported for one cell line that serum deprived of CIg by passage over immobilized gelatin is deficient in normal cell spreading [44]. As discussed earlier, CIg adsorbed from the medium can be detected by immunofluorescence, but by SDS-PAGE analysis CIg seems to be a minor component of the proteins adsorbed to the substratum [Haas and Culp, in preparation].

Since substratum-bound CIg probably represents the primary site of interaction between cellular adhesive material and the substratum, SAM produced on substrata coated with purified CIg should resemble SAM produced in the usual manner on serum-coated substrata. SDS-PAGE analysis shows that this is, in fact, the case [Murray and Culp, in preparation]. SAM from cells attaching on CIg-coated substrata contains as much cellular fibronectin as SAM from cells attaching to serum-coated substrata. This suggests that CIg in the serum layer cannot functionally substitute for cell surface fibronectin. This interpretation is supported by the finding that cell-surface fibronectin and high molecular weight proteoglycans are the major iodinatable cell-surface components incorporated into new adhesion sites when cells are prelabled with ^{131}I by the lactoperoxidase technique, removed with EGTA, and allowed to reattach onto a fresh substratum before preparing SAM; in contrast, the released cells themselves contain many iodinated species by SDS-PAGE [Cathcart and Culp, in preparation]. Even though these cells retain surface-iodinated fibronectin, they still require substratum-bound CIg for normal attachment and spreading.

Furthermore, when cells are removed by trypsin treatment under conditions that remove all surface-associated fibronectin and are allowed to attach to fresh substrata, the SAM that is laid down contains normal amounts of metabolically labeled (cell-derived) fibronectin [Buniel and Culp, unpublished results]; this presumably derives from intracellular or newly synthesized fibronectin.

Interestingly, the *quantity* of ^{3}H-glucosamine-polysaccharide retained when pre-labeled SVT2 cells are allowed to reattach to a substratum for 1 h before they are removed is considerably greater when the substratum was precoated with purified CIg rather than with serum. SVT2 cells on CIg-coated substrata also spread more extensively than they do on the serum-coated substrata.

Glycosaminoglycans in SAM

A role for complex carbohydrates in cell adhesion has been postulated on the basis of evidence from a wide variety of studies [reviewed in reference 1]. The molecular structure of these carbohydrates is unclear, but much attention has been focused on glycoproteins, and, in particular, on fibronectin, as described earlier [3, 11, 21, 46–49]. Considerable attention also has been paid to cell surface glycosaminoglycans (GAGs), but most of these experiments have yielded only indirect evidence for an adhesive role for GAGs.

A promising line of investigation was begun when it was discovered that SAM is highly enriched for GAGs when compared to the rest of the cell [11, 16, 52]. Initially, only hyaluronic acid was chemically identified in SAM [16]. Metabolic radiolabeling with $^{35}SO_4$, however, revealed the presence of sulfated GAG [16, 52], and when glucosamine- or sulfate-radiolabeled SAM was analysed by SDS-PAGE, nearly all of the radioactivity was found in three high molecular weight GAG-associated bands [11].

The GAGs in SAM have since been examined in greater detail and have been compared with the GAGs in the rest of the cell [12]. We hoped that a specific redistribution of the GAGs in SAM would suggest their functional role(s) in adhesion. Table I shows the distribution of radioactivity among the various GAGs and glycopeptide in the cell-associated, EGTA-soluble, and substrate-attached material of 3T3 cells after exposure to ^{3}H-glucosamine for 72 h. Both EGTA-soluble material and SAM are relatively enriched for GAG.

The distribution of specific GAGs in this preparation from 3T3 cells (and SVT2 cells, not shown) reveals several patterns. Essentially, the relative amounts of chondroitin 4-sulfate and unsulfated chondroitin rise in SAM as compared to cell-associated material, whereas the relative amount of dermatan sulfate falls. These rises and falls are reproducible. Also, the rise and fall in the relative amount of heparan sulfate in the various fractions tends to be paralleled by the changes in amount of glycopeptide in the same fractions.

Thus it is apparent that GAGs are redistributed in cellular adhesion sites. This does not in itself demonstrate functionality for the GAGs, and so we compared SAM from cells adherent for only 1 h (before they begin to spread) to SAM from cells adherent for 72 h (during which time they move several cell diameters [53], leaving a SAM enriched for footprints). Table II shows the distribution of radioactivity in polysaccharides from these preparations in 3T3 cells. Results for SVT2 cells were similar. The most striking result is the enrichment for heparan sulfate in newly formed footpads. It is almost three times the amount seen in footprint-enriched SAM. This parallels the large rise in radiolabeled glycopeptide content in SAM from these reattaching cells. That these changes are occurring *specifically* at the footpad is indicated by the similarity between the *cell-associated* GAG distributions in long-term radiolabeled and reattaching cells.

In summary, newly formed adhesion sites are highly enriched for heparan sulfate and

TABLE I. Distribution of Long-Term Radiolabeled Polysaccharides in 3T3 Cells*

Polysaccharide[a]	% Radioactivity[b]			
	Cell-associated	EGTA-soluble	Cell+EGTA[c]	Substrate-attached
Glycopeptide	73.6	36.0	72.7	27.9
GAG	26.4	64.0	27.3	72.1
Total	100.0	100.0	100.0	100.0
HS	48.8	22.2	48.2	26.3
6S	0.8	1.1	0.8	2.3
4S	5.7	8.3	5.8	22.4
DS	24.0	11.7	23.7	2.7
OS	3.1	18.0	3.5	23.6
HA	17.6	38.7	18.0	22.7
Total	100.0	100.0	100.0	100.0

*Analytical procedures have been described by Rollins and Culp [12]. Briefly, cultures of 3T3 cells were labeled for 72 h with ^{3}H-glucosamine, following which the cells were detached by EGTA treatment. Substrate-attached polysaccharide is material resistant to EGTA-mediated release; cell-associated polysaccharide is material that is found in the washed pellet after a low-speed centrifugation; and EGTA-soluble polysaccharide is material that remains in the supernatant after the low-speed centrifugation. Polysaccharides were isolated by ethanol precipitation of Pronase-digested fractions. Hyaluronic acid, dermatan sulfate, and the chondroitins were identified and quantitated by paper chromatography of chondroitinase AC and chondroitinase ABC digests. Heparan sulfate and glycopeptide were identified and quantitated by Sepharose CL-6B chromatography of chondroitinase ABC digests; heparan sulfate was measured as material sensitive to nitrous acid degradation.

[a]HS, heparan sulfate; 6S, chondroitin 6-sulfate; 4S, chondroitin 4-sulfate; DS, dermatan sulfate; OS, unsulfated chondroitin; HA, hyaluronic acid.

[b]Glycopeptide and GAG are shown as the percentage of total polysaccharide radioactivity, whereas the individual GAGs are shown as the percentage of total GAG radioactivity.

[c]The precentage of radioactivity in the (cell + EGTA) fractions contained in a specific polysaccharide was determined as follows:

$$\% \text{ radioactivity} = \frac{\text{(cpm of specific polysaccharide in cell-associated and EGTA-soluble material)}}{\text{(cpm of total polysaccharide in cell-associated and EGTA-soluble material)}} \times 100$$

depleted of hyaluronic acid and the chondroitins, as compared to the rest of the cell. As the adhesion sites mature – ie, as the cells begin to spread – there is a progressive accumulation of unsulfated chondroitin and hyaluronic acid in a fairly constant proportion. This accumulation occurs *coordinately* and *specifically* at the adhesion site, suggesting that the chondroitins and hyaluronic acid may be somehow associated with each other. This situation is reminiscent of the hyaluronate-chondroitin proteoglycan complexes in cartilage [54–56].

Proteoglycans in SAM

Most glycosaminoglycans are found as parts of large proteoglycans [56, 57]. We devised techniques to analyze intact GAG-containing molecules from SAM. The effect of

TABLE II. Distribution of Radiolabeled Polysaccharides in SAM From Long-term Radiolabeled and Reattaching Cells*

Cellular fraction	Polysaccharide[a]	% Radioactivity[b] Long-term	Reattaching
Cell-associated	Glycopeptide	73.6	59.7
	GAG	26.4	40.3
	Total	100.0	100.0
	HS	48.8	56.8
	6S	0.8	2.5
	4S	5.7	4.3
	DS	24.0	17.7
	OS	3.1	2.5
	HA	17.6	16.2
	Total	100.0	100.0
SAM	Glycopeptide	27.9	66.6
	GAG	72.1	33.4
	Total	100.0	100.0
	HS	26.3	80.2
	6S	2.3	1.6
	4S	22.4	8.0
	DS	2.7	0.9
	OS	23.6	4.8
	HA	22.7	4.5
	Total	100.0	100.0

*3T3 cells were grown in the presence of ^{3}H-glucosamine for 72 h as described in Table I (long-term), and the polysaccharides were analyzed for radioactivity. Alternatively, long-term radiolabeled cells were removed from dishes with EGTA, washed in cold PBS, and replated in fresh dishes. After 1 h SAM polysaccharides were analyzed as usual (reattaching).

[a]HS, heparan sulfate; 6S, chondroitin 6-sulfate; 4S, chondroitin 4-sulfate; DS, dermatan sulfate; OS, unsulfated chondroitin; HA, hyaluronic acid.

[b]Glycopeptide and GAG are shown as the percentage of total polysaccharide radioactivity, whereas the individual GAGs are shown as the percentage of total GAG radioactivity.

proteolytic treatment of these species was then assessed in an attempt to demonstrate the existence of proteoglycans [Rollins and Culp, in preparation].

The carbohydrate-containing species of SAM were initially separated by molecular sieve chromatography on Sepharose CL-2B in an SDS buffer. The resulting profile from a preparation doubly labeled with $^{35}SO_4$ and ^{3}H-glucosamine is shown in Figure 6. Three classes of glucosamine-labeled material were resolved, of which two (areas II and III) were sulfated. The profile was not altered by omission of protease inhibitors or by reduction and alkylation of SAM before analysis. Similar results were seen with SAM from 3T3 or SVT2 cells.

SAM was also electrophoresed in SDS buffer on 1.5–10% concave logarithmic polyacrylamide gels containing 1% agarose for structural support (Fig. 7A). The three areas separated by electrophoresis correspond to the three areas of SAM separable by gel chromatography (Fig. 7B–D). The material of highest apparent molecular weight migrates as a relatively sharp band and is not labeled with $^{35}SO_4$ or ^{14}C-leucine (data not shown).

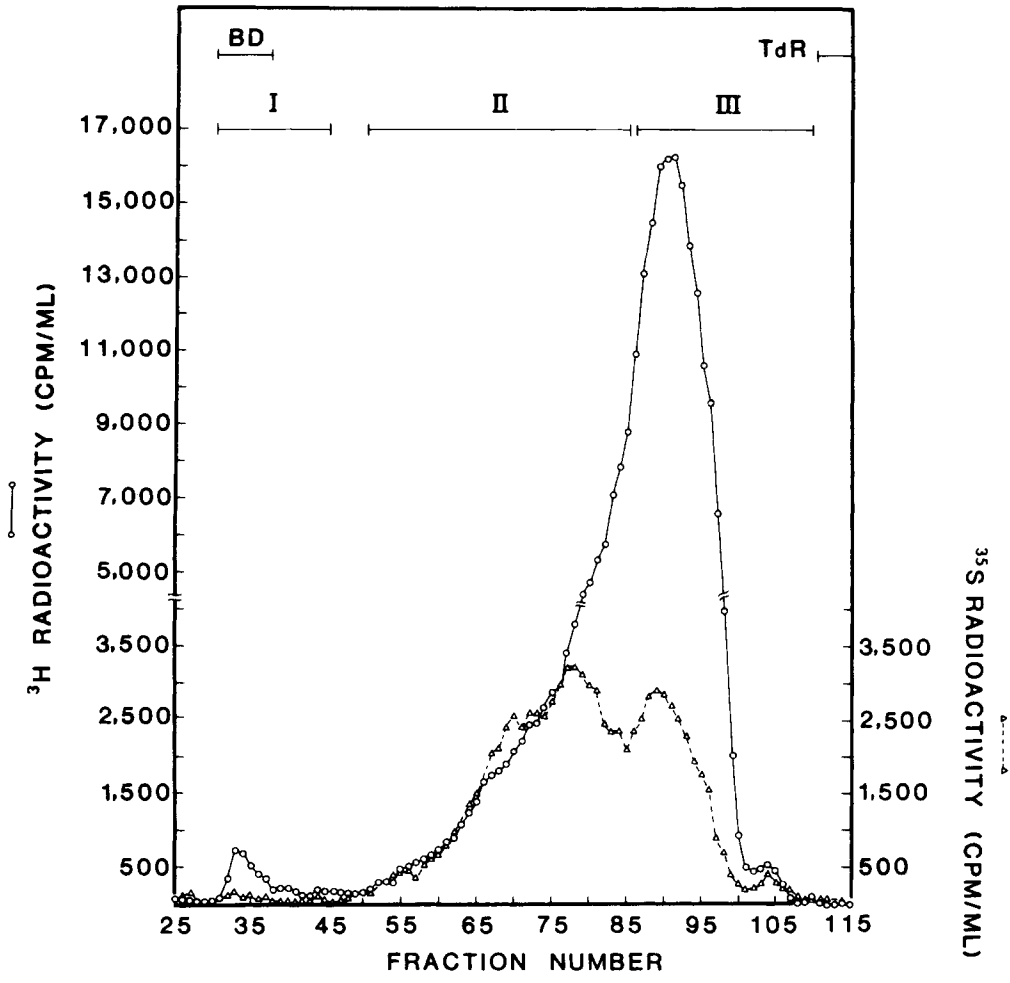

Fig. 6. SDS chromatography on Sepharose CL-2B of SAM from long-term ^{3}H-glucosamine, $^{35}SO_4$ radiolabeled SVT2 cells. SVT2 cells were grown for 72 h in the presence of ^{3}H-glucosamine and $Na_2{}^{35}SO_4$ and then removed with EGTA (containing PMSF). The SAM was extracted with SDS (also containing PMSF) and, after vacuum dialysis, it was chromatographed on a column of Sepharose CL-2B (1 X 120 cm, eluted with 120 mM Tris-HCl (pH 7.4), 0.2% SDS) [Rollins and Culp, Biochemistry, in press].

The other two ^{14}C-glucosamine-labeled areas are diffuse and the areas are not well separated. Both are labeled by $^{35}SO_4$ and ^{14}C-leucine. Similar patterns were seen for SVT2 cell SAM.

In order to identify the proteoglycans in SAM, the areas of radioactivity shown in Figure 6 were analyzed for carbohydrates before and after Pronase digestion. Such analysis has shown that the material in area I of Figure 6 is entirely composed of hyaluronic acid, the eluted position of which does not change after Pronase digestion. Area II is composed of the other GAGs, along with some glycopeptide. Digestion of this material with Pronase showed that all of the chondroitin species and some 50% of the heparan sulfate species are structurally attached to protein as defined by a change in column elution position after Pronase digestion. Analysis of area III, which contained the rest of the GAG along with

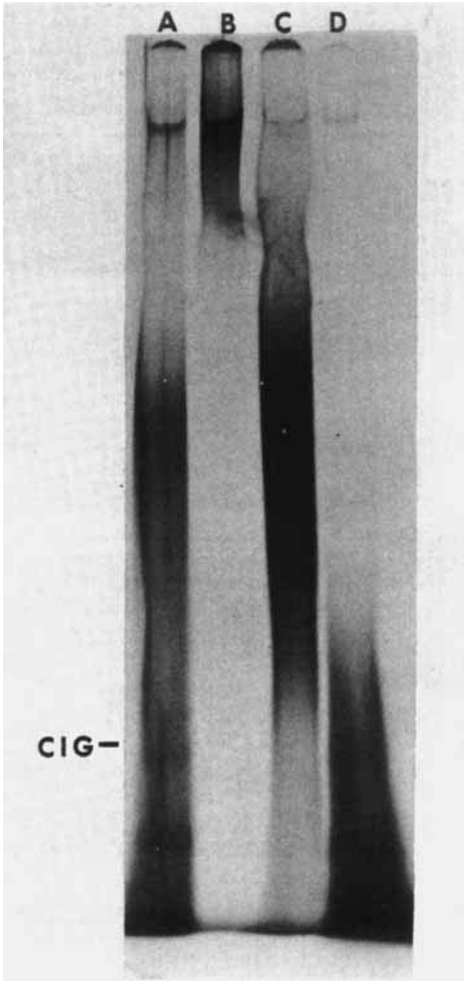

Fig. 7. SDS-PAGE on gradient gels of chromatographically fractionated SAM from long-term radiolabeled 3T3 cells. An aliquot of SDS-extracted SAM from long-term ^{14}C-glucosamine radiolabeled 3T3 cells was electrophoresed on a 1.5–10% concave logarithmic polyacrylamide gel containing 1% agarose. Another aliquot was chromatographed on Sepharose CL-2B as described in the legend to Figure 6. The indicated areas in Figure 6 were collected and electrophoresed on the same gel as the unfractionated SAM: well B, area I; well C, area II; well D, area III. The position of human CIg after electrophoresis is indicated [Rollins and Culp, Biochemistry, in press].

much glycopeptide, yielded essentially similar results. Table III (based on unpublished data of Rollins and Culp) summarizes the proteoglycan species thus far identified in SAM on the basis of their apparent hydrodynamic sizes before and after Pronase digestion.

Association of SAM Proteoglycans

In order to assess the ability of SAM proteoglycans to interact with each other, or with other components in SAM, we adapted some techniques used in cartilage research [56, 58, 59] for use with SAM (Fig. 8) [Rollins and Culp, in preparation]. When a 4.0 M guanidine hydrochloride extract of long-term ^{3}H-glucosamine/$^{35}SO_4$ radiolabeled SAM is

TABLE III. Proteoglycan and GAG Species in SAM*

Radiolabeling conditions	Species[a]	Comments
Long-term	HA	No detectable protein, largest apparent molecular weight
	4S-6S-OS	Larger molecular weight proteoglycan, present in large amounts
	4S-OS	Smaller molecular weight proteoglycan, present in small amounts
	HS	Proteoglycan
	DS	Proteoglycan
Reattaching	HA	No detectable protein
	6S-OS	Largest proteoglycan in reattaching cell SAM
	4S-OS	Smaller molecular weight proteoglycan
	HS	Proteoglycan
	DS	Probably not in proteoglycan form

*These species are tentatively identified by their behavior on gel chromatography before and after Pronase digestion (see text).
[a]HS, heparan sulfate; 6S, chondroitin 6-sulfate; 4S, chondroitin 4-sulfate; DS, dermatan sulfate; OS, unsulfated chondroitin; HA, hyaluronic acid. Species are named by the carbohydrate components they contain.

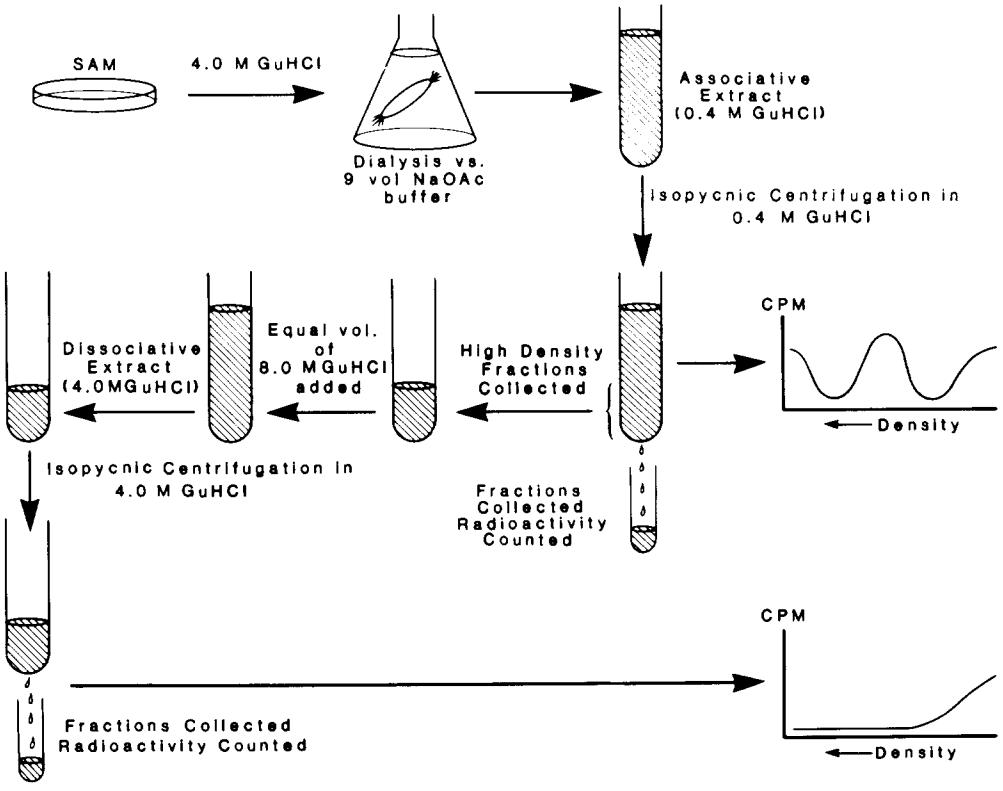

dialyzed to associative conditions (0.4 M guanidine hydrochloride) and centrifuged to equilibrium in a cesium chloride gradient, the profile of Figure 9A results. There are two major peaks of radioactivity at densities greater than 1.580 g/ml. The denser peak, at the bottom of the gradient, has a much higher ratio of ^{35}S to ^{3}H radioactivity than does the peak of intermediate density. There is also a small area of ^{35}S and ^{3}H radioactivity at the top of the gradient.

When the material banding at densities greater than 1.580 g/ml (fractions 1–8, Fig. 9A) is brought to dissociative conditions (4.0 M guanidine hydrochloride) and again centrifuged to equilibrium in cesium chloride, the radioactivity is distributed as shown in Figure 9B. Although small amounts of ^{35}S and ^{3}H radioactivity are at the bottom of the gradient, over 80% of the ^{3}H and 75% of the ^{35}S radioactivity bands at densities less than 1.580 g/ml. This material can be dialyzed to 0.4 M guanidine hydrochloride and recentrifuged to give the same pattern as fractions 1–8 in Figure 9A (data not shown). Thus the carbohydrates in SAM are capable of undergoing a reversible association into highly negatively charged aggregates.

The material at the bottom of the gradient (fractions 1 and 2, Fig. 9A), comprising only 6% of the total radioactivity, is over 80% GAG. Of this GAG, about 40% is heparan sulfate, and the rest is chondroitinase ABC–digestible material. The band of intermediate density (fractions 3–9) is over 80% heparan sulfate and comprises 31% of the total radioactivity. There is also a small amount of other GAG and glycopeptide in this fraction. Thus the high-density material is qualitatively different from the intermediate-density material (both by analysis here and by ^{35}S:^{3}H ratios in Figure 9A), but both areas are capable of being disaggregated by 4.0 M guanidine hydrochloride. The least dense fractions (10–12), with 14% of the total radioactivity, have nearly equal amounts of heparan sulfate and glycopeptide and are slightly depleted of glycopeptide.

The material sticking to the centrifuge tube (routinely 48% of the total radioactivity) is highly enriched for chondroitinase-digestible GAG. A smaller amount of glycopeptide and even less heparan sulfate also stick to the tube. No radioactivity was found adherent to any of the other surfaces used in these experiments (eg, dialysis tubing).

In order to assess the role of intact protein in the observed aggregation phenomenon, SAM was tested for its ability to aggregate after extensive protease digestion. A typical associative sedimentation equilibrium analysis of long-term radiolabeled SVT2 cell SAM is shown in Figure 10A. Fractions 1–9 were combined and digested for 24 h with Pronase in the presence or absence of SDS. This material was extensively dialyzed, then made 0.4 M in guanidine hydrochloride and centrifuged under these associative conditions. This treatment had little effect on the aggregation of the intermediate-density material

---

Fig. 8. Isopycnic centrifugation of SAM under associative and dissociative conditions. Radiolabeled cells were removed from dishes with EGTA, and the SAM remaining on the dishes was extracted with 4.0 M guanidine hydrochloride in 0.054 M sodium acetate (pH 5.8) at 4°C for 48 h. The extract was dialysed against 9 vol 0.05 M sodium acetate to reduce the concentration of guanidine hydrochloride to 0.4 M. These are defined as associative conditions [56]. The associative extract was brought to a loading density of 1.63 g/ml cesium chloride and centrifuged in a Beckman 50 Ti rotor at 34,000 rpm at 18°C for 48 h. After centrifugation, 1 ml fractions were collected by piercing the bottom of the centrifuge tube, and the density and radioactivity of each sample was determined. The lower two-thirds of the associative gradient was brought to dissociative conditions (4.0 M guanidine hydrochloride), cesium chloride was added to a density of 1.54 g/ml, and centrifugation and analysis of the gradient were performed as described for the associative gradients.

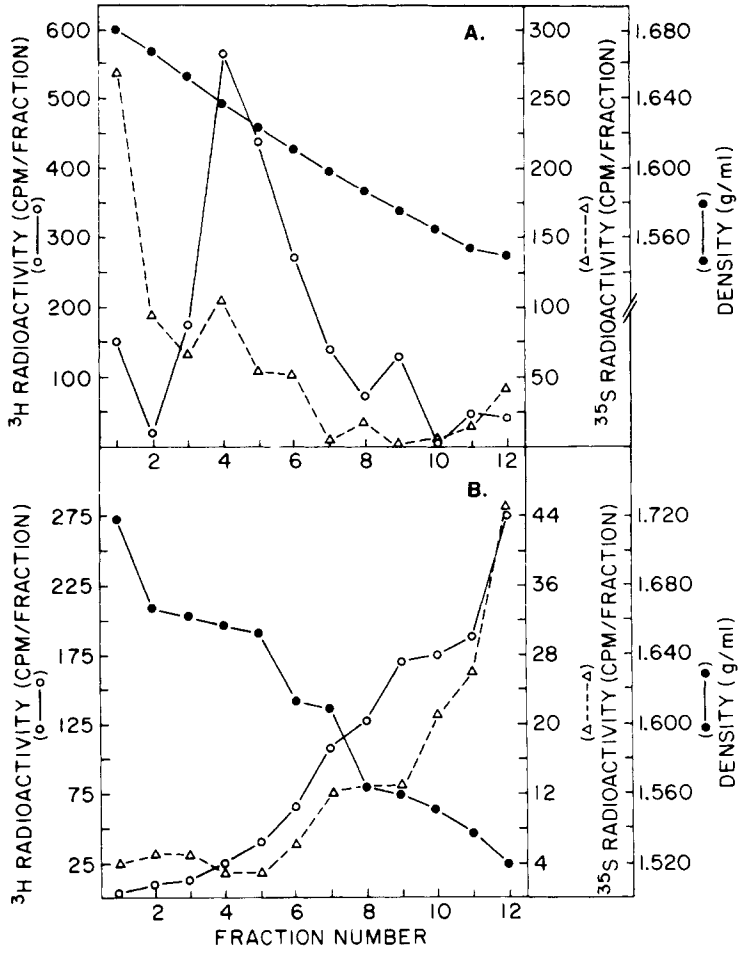

Fig. 9. Associative and dissociative isopycnic centrifugation of SAM from long-term ^{3}H-glucosamine, $^{35}SO_4$ radiolabeled 3T3 cells. SAM from long-term ^{3}H-glucosamine/$^{35}SO_4$ radiolabeled 3T3 cells was extracted with 4.0 M guanidine hydrochloride, concentrated, and dialyzed to 0.4 M guanidine hydrochloride as described in Figure 8. Cesium chloride was added to this extract to a density of 1.63 g/ml and the mixture was centrifuged to equilibrium (A). Fractions 1–8 from A. were combined and made 4.0 M in guanidine hydrochloride. Cesium chloride was added to a density of 1.54 g/ml, and the mixture was centrifuged to equilibrium (B). Approximately 1 ml fractions were collected from the bottoms of the centrifuge tubes and the density (–●–●–), ^{3}H (–○–○–), and ^{35}S (–△–△–) radioactivity of each fraction were determined as described in Figure 8 [Rollins and Culp, Biochemistry, in press].

(fractions 3–7) but altered the appearance of the densest aggregate (fractions 1–2) (see Fig. 10B). This effect, although slight, was observed reproducibly in several experiments.

In cartilage [56], hyaluronic acid is a multivalent ligand, binding several proteoglycan subunits along its length. To assess the possible multivalency of hyaluronic acid in SAM, an aliquot of combined fractions 1–9 in Figure 10A was dissociated by adding an equal volume of 8.0 M guanidine hydrochloride. To this dissociated mixture was added 100 μg of HA-80, a hyaluronidase digestion product from hyaluronic acid consisting of approximately 80 repeating units. The size of this oligomer (a maximum of 0.003% of the size of

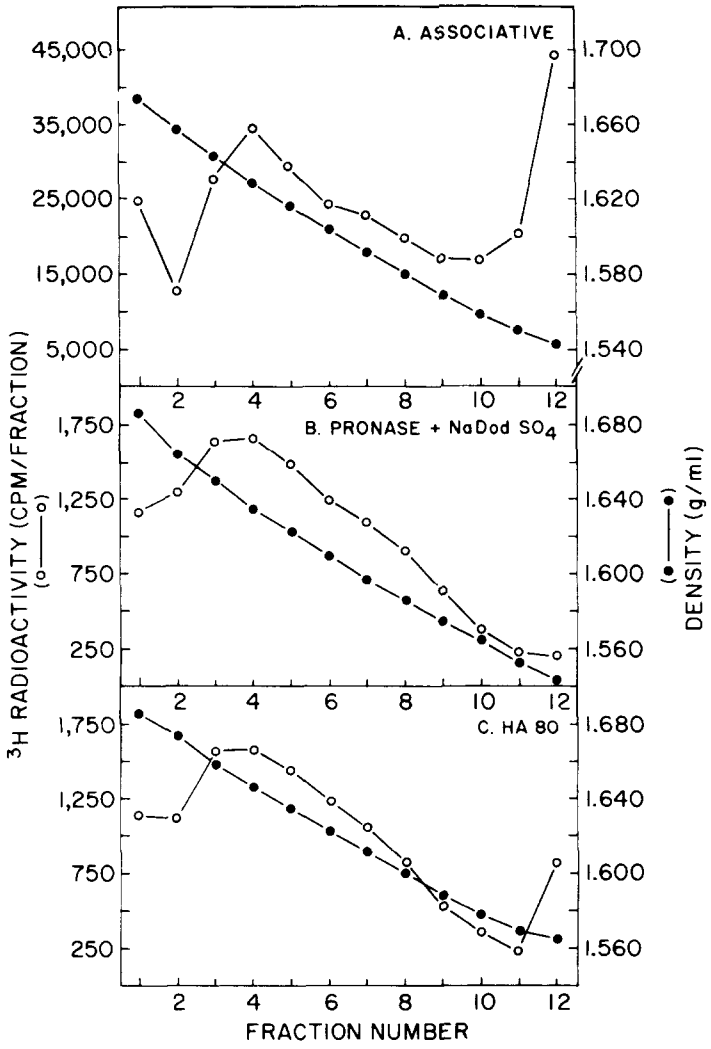

Fig. 10. Effect of Pronase digestion and HA80 on the behavior in isopycnic centrifugation of SAM from long-term ^{3}H-glucosamine radiolabeled SVT2 cells. SAM from long-term ^{3}H-glucosamine radiolabeled SVT2 cells was extracted with 4.0 M guanidine hydrochloride, dialyzed to associative conditions, and centrifuged to equilibrium in cesium chloride (A). Fractions 1–9 of this associative gradient were digested with Pronase and recentrifuged under associative conditions to give a profile indistinguishable from that seen in fractions 1–9 in A. This material was divided into two aliquots. One aliquot was made 0.2% in SDS and redigested with Pronase. This digest was dialyzed and recentrifuged (B). The other aliquot was made 4.0 M in guanidine hydrochloride, 100 μg HA80 were added, and the mixture was then dialyzed back to 0.4 M guanidine hydrochloride and recentrifuged (C). Fractions were collected and their densities (–•–•–) and content of ^{3}H radioactivity (–o–o–) were measured as described in Figure 8 [Rollins and Culp, Biochemistry, in press].

most of the hyaluronic acid in SAM) corresponds to the distance between attached proteoglycan subunits in the cartilage aggregate [56].

The dissociative mixture was kept at 4°C for 24 h, then dialyzed against 9 volumes of buffer to bring it back to associative conditions. This mixture was centrifuged as usual, and the result is shown in Figure 10C. A little less than 10% of the total radioactivity was found in the least dense fraction of the gradient, indicating a competitive effect of the HA-80 on aggregate formation. This effect was observed reproducibly in several experiments. This suggests that the HA-80 may have competed against cartilage-like aggregate formation in the higher density area of the gradient.

In cartilage, it has been elegantly shown that the formation of the protein–polysaccharide complex is due to interaction of the core protein of the chondroitin-keratin proteoglycan subunit with hyaluronic acid (an interaction further stabilized by another glycoprotein) [56–58]. All of the elements of the cartilage aggregate system (except the glycoprotein link) have been shown to be present in these lower gradient fractions of guanidine-extracted SAM. Furthermore, the addition of HA-80 to presumably aggregated material leads to the displacement of some of the formerly aggregated material from the densest gradient fractions. These results suggest, but by no means demonstrate, that a small proportion of the macromolecular aggregates in SAM may resemble cartilage proteoglycan aggregates. We are now examining this possibility by further experimentation.

The majority of complex formation in SAM, however, seems to be somewhat independent of the presence of intact protein. The behavior of the intermediate density fractions of SAM in isopycnic centrifugation is not altered by Pronase digestion either in the absence or the presence of SDS. The other major difference from the cartilage system is the striking enrichment for heparan sulfate in this intermediate-density material. Over 82% of all the carbohydrate in the fractions of density between 1.600 g/ml and 1.660 g/ml is heparan sulfate. The fact that 4.0 M guanidine hydrochloride can force nearly all of this material to band at densities less than 1.600 g/ml suggests that SAM contains polysaccharides that have the potential to form aggregates consisting mostly of heparan sulfate. Whether the heparan sulfate is combining with itself and/or other components to form these aggregates cannot be determined from these experiments.

The existence of aggregates in the high-density fractions of these associative gradients has not been rigorously demonstrated by this work. There are, however, precedents specifically involving heparin derivatives. Macromolecular heparin from rat skin [60] and native heparin from rat peritoneal mast cells [61] have been shown to be large molecular weight proteoglycans (1.1×10^6 mol wt and 750,000 mol wt, respectively) which are resistant to protease digestion (including Pronase) but are degraded to free carbohydrate chains by alkali and can be shown to contain xylose and serine. Thus the heparan sulfate in SAM could be engaging in protein-mediated interactions with itself or other components, and yet this protein would remain insensitive to protease treatment.

Alternatively, the observed aggregation phenomenon could be due to carbohydrate–carbohydrate interaction. If these interactions are mediated by hydrogen bonds, or if they depend in some way on specific conformations of the polysaccharides (some of which are known to be hydrogen bond-directed [57]), then guanidine hydrochloride should be able to disrupt the interactions by its ability to disrupt hydrogen bonding.

That SAM is not identical to cartilage is not surprising. The suggested interactions involving the heparan sulfate of SAM are, however, unique since, until now, no tissue system has been described in which "macromolecular" heparan sulfate of heparan sulfate

proteoglycans are known to play a role. Whether this phenomenon is functionally related to the enrichment for heparan sulfate in the early adhesion site is unknown.

Protein–Polysaccharide Interrelationships in SAM

To examine further the structural and functional relationships between the various components of SAM, we have carried out digestion experiments with trypsin and hyaluronidase [15]. Trypsinization of SAM with purified TPCK-trypsin at low concentrations (1–10 μg/ml) for 15 min releases 70–80% of the ^{3}H-glucosamine-labeled polysaccharide but only 35–45% of the ^{3}H-leucine-labeled protein. Previous work has shown that most of the ^{3}H-glucosamine-labeled material in SAM is glycosaminoglycan [16]. These results were typical of both 48-hour-labeled (long-term) and 2-hour-labeled (short-term) SAM. Chemical analysis revealed that trypsinization selectively solubilizes hyaluronate and the chondroitins, whereas heparan sulfate is quite resistant to solubilization. Also, heparan sulfate in SAM is not exchangeable with exogenously added heparin [Culp, unpublished data], in contrast to the exchangeability observed for heparan sulfate on other regions of the cell surface [45].

SDS-PAGE analysis of the trypsin-resistant material from these cultures (Fig. 11) revealed that only a few leucine-labeled bands are selectively labile to trypsin treatment. The large GAP-1 band is lost selectively from both long-term and short-term preparations, even at very low trypsin concentrations (1 μg/ml); this band is associated chiefly with the chondroitins [15].

Fibronectin in SAM is not selectively labile to trypsin in long-term radiolabeled preparations, in contrast to the fibronectin found on other regions of the cell surface [2]; however, the metabolically labile, pulse-radiolabeled (short-term) fibronectin in this adhesive material is selectively labile to digestion. Consistent with this, the fibrillar pattern of immunofluorescence of fibronectin in SAM, which would be expected to reflect the properties chiefly of the more abundant, long-term radiolabeled fibronectin, is resistant to trypsin digestion under the conditions used here [Murray and Culp, unpublished data]. These results suggest that most of the fibronectin in SAM is contained within a highly resistant adhesive structure rich in heparan sulfate; however, *newly synthesized* fibronectin is present in a much more labile structure, along with hyaluronate and the chondroitins. Upon chasing pulse-radiolabeled cells with cold leucine before preparing SAM, some but not all of this fibronectin becomes incorporated into the resistant material [12, 15], again demonstrating the process of maturation that the adhesion sites undergo. However, these experiments could not address the question of the nature of the interaction between the fibronectin and the respective glycosaminoglycans, if any, since there are many other proteins in SAM whose digestion might disrupt a labile structure, releasing glycosaminoglycans and fibronectin.

We then turned to digestion with testicular hyaluronidase, which will digest hyaluronic acid and the chondroitins but not heparan sulfate. Hyaluronidase solubilized about half of the labeled polysaccharide in long-term or short-term labeled SAM, consistent with the glycosaminoglycan content of these preparations, but digested only 10–15% of the polysaccharide from reattaching-cell SAM, consistent with the high heparan sulfate content of this material. Hyaluronidase treatment released only about 10–15% of the labeled protein from long-term radiolabeled preparations, about 5% from short-term preparations, and almost none from reattachment preparations. Protein patterns on SDS-PAGE of resistant and soluble material from long-term labeled SAM are very similar to each other and to the

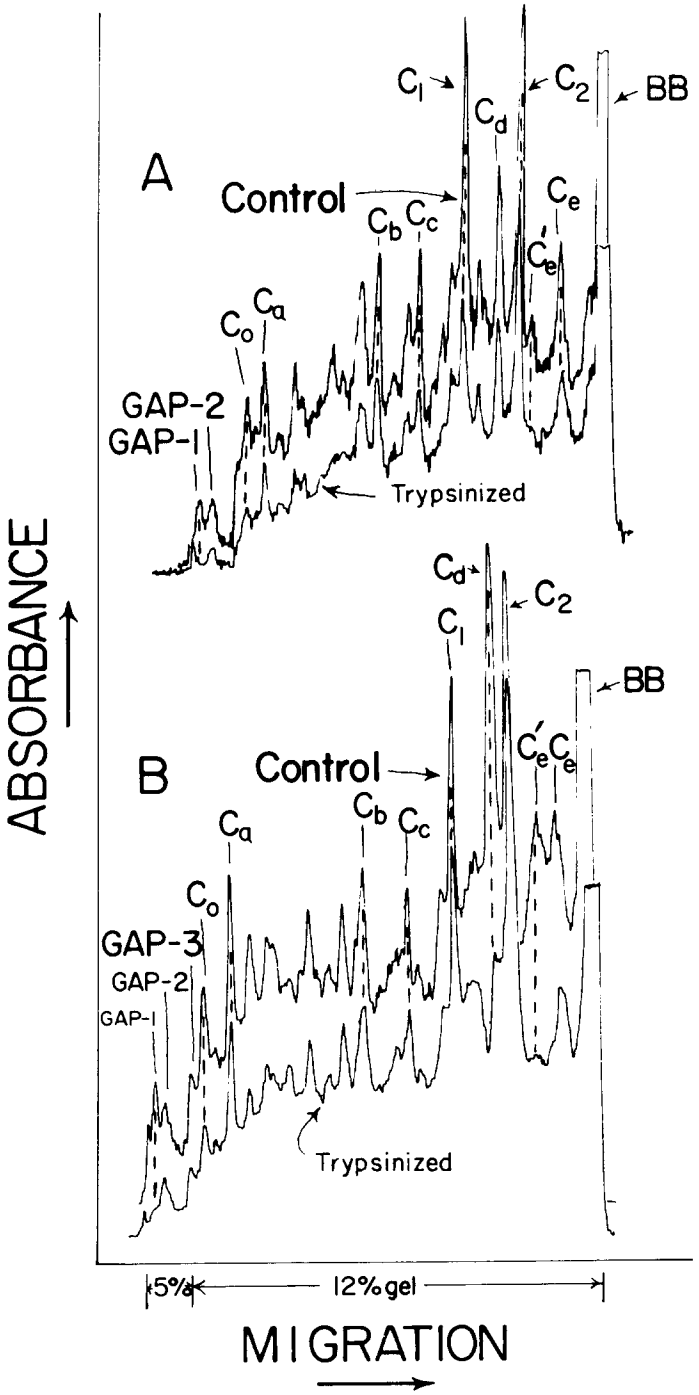
A
Control
C_1
C_d
C_2
BB
C_e
C_b C_c
C'_e
C_o C_a
GAP-2
GAP-1
Trypsinized
B
Control
C_d
C_1
C_2
BB
C'_e C_e
C_a
C_b C_c
C_o
GAP-3
GAP-2
GAP-1
Trypsinized
ABSORBANCE
5%
12% gel
MIGRATION

11

pattern of undigested material, with perhaps a slight enrichment in the C_0 band (fibronectin) in the released material. This may reflect a small amount of newly synthesized fibronectin in long-term labeled material (see below). Only small quantities (10% or less) of heparan sulfate, fibronectin, and cytoskeletal protein were solubilized under conditions which solubilized greater than 90% of the hyaluronate and the chondroitins [15]. Furthermore, immunofluorescence microscopy also showed that the (long-term) fibronectin in SAM is resistant to hyaluronidase digestion [Murray and Culp, unpublished data]. Interestingly, in short-term labeled material, the C_0 band was specifically and completely released by hyaluronidase digestion, and no radiolabeled cytoskeletal protein was released under these conditions.

Thus newly synthesized fibronectin is bound to SAM by a hyaluronidase-sensitive structure, perhaps in a cartilage-like proteoglycan, as discussed above. Unfortunately, because of the difficulty of obtaining heparan-sulfate-digesting enzymes of sufficient specificity and purity, we have not yet been able to carry out a similar analysis for the hyaluronidase-resistant heparan-sulfate-containing material.

A Model for Cell-Substratum Adhesion

The foregoing data and discussion suggest a tentative model of adhesion and a description of the molecular events occurring within the adhesion site (Fig. 12). During the early adhesive interaction with the substrate (< 1 h), no cell spreading has occurred, and the dependence of this interaction on metabolic activity or cytoskeletal function is minimal [18]. It is also during this period that SAM is strikingly enriched for heparan sulfate. The fact that heparin binds strongly and specifically to CIg [7] suggests that this initial adhesive interaction may involve cell-surface heparan sulfate acting as a cross-link between the cell-surface fibronectin [11, 62], and substrate-bound CIg (Fig. 12A). This correlates with all of the experimental indications to date that the cell-adhesion and spreading factor found in serum is CIg, as discussed earlier.

Over 72 h an accumulation of certain proteoglycan species occurs specifically in the adhesion site. There is a relative increase in the proportion of hyaluronic acid and of proteoglycans containing the galactosaminoglycans (dermatan sulfate and the chondroitins). (For concreteness, the proteoglycans in the model of Figure 12 are depicted as complexes analogous to the proteoglycans found in cartilage [56, 57], but as discussed earlier, this form of organization is by no means established for the SAM proteoglycans.) This accumulation could be the chemical reflection of the physiological maturation that the footpad undergoes as it loosens its connections with the cell body to become a footprint [1, 63]. The mechanism whereby such an accumulation of polysaccharide might weaken the foot-

---

Fig. 11. SDS-PAGE analyses of trypsin-treated SAM. SAM was prepared from SVT2 cultures grown for 48 h (A) or 2 h (B) in radioactive leucine-containing medium. Control preparations received no trypsin, whereas trypsinized preparations were treated with 5 μg/ml for 15 min at 37°C. Trypsin activity was destroyed with soybean trypsin inhibitor and PMSF and SAMs were isolated for SDS-PAGE analyses as described elsewhere [11, 15]. 10,000 cpm of SAM of control (48 h), control (2 h), and trypsinized (2 h) samples were electrophoresed in adjacent wells of a slab gel, whereas only 6,000 cpm of the trypsinized (48 h) sample was used; the gel was fluorographed. Various proteins are identified in the legend to Figure 2 or in the text. Treatment with trypsin concentrations varying between 0.25 and 10 μg/ml generated the pattern differences shown here (reprinted from reference 15 with permission of the publisher).

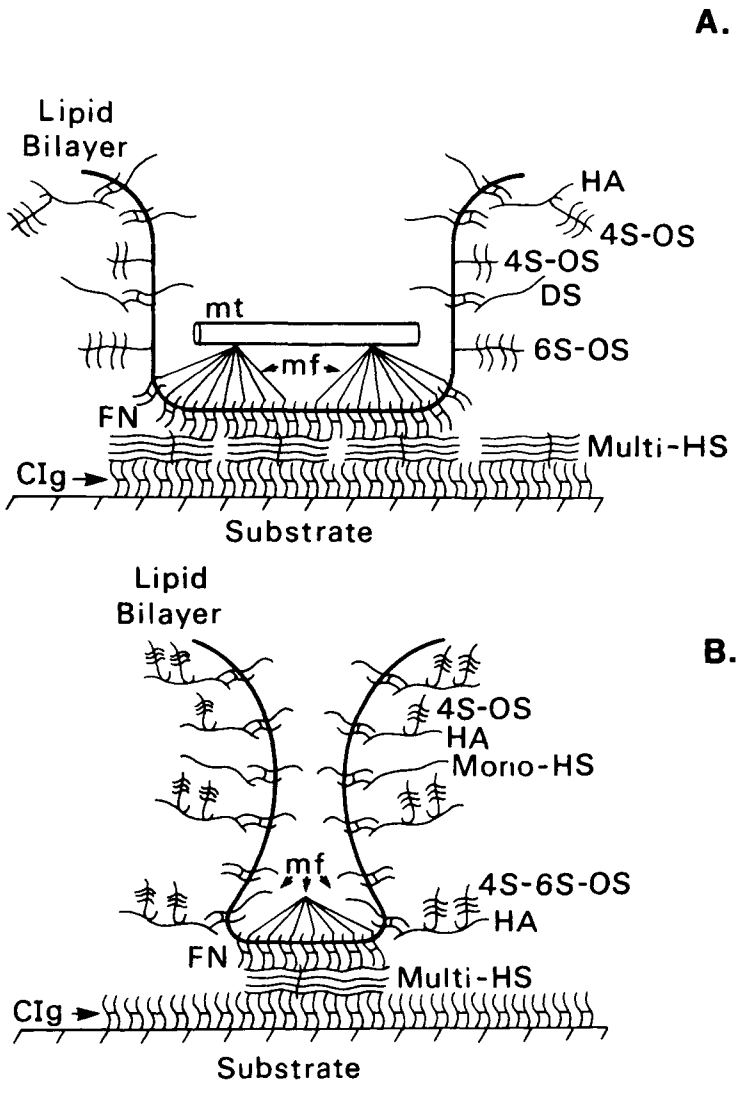

Fig. 12. Model of cell-substrate adhesion. Identifiable components of a single footpad are shown in the newly formed adhesion site of reattaching cells (A) and in the fully matured adhesion site just before the cell breaks its connection with the footpad (B). See text for details. Multi-HS, macromolecular or proteoglycan heparin sulfate multivalent for fibronectin; mono-HS, heparin sulfate chains monovalent for fibronection; FN, fibronectin; CIg, cold-insoluble globulin; 6S-OS, undersulfated chondroitin 6-sulfate proteoglycan; 4S-OS, undersulfated chondroitin 4-sulfate proteoglycan; 4S-6S-OS, incompletely sulfated chondroitin 4-sulfate and chondroitin 6-sulfate proteoglycan; DS, dermatan sulfate; HA, hyaluronic acid; mf, microfilaments; mt, microtubule.

pad remains obscure, but a suggested model is shown in Figure 12B. If hyaluronic acid and the galactosaminoglycan-containing proteoglycans are monovalent in their interaction with fibronectin, then during their accumulation in the adhesion site, they may be able to compete with multivalent heparan sulfate for binding to fibronectin. Monovalent heparan sulfate chains could act in the same manner. If fibronectin is connected in some wasy to the cell's

cytoskeletal apparatus [41], such a competition could lead to a localized destabilization of this apparatus and subsequent pinching off of the footpad.

There are several examples of systems in which stimuli for cell growth, movement, and detachment are correlated with hyaluronic acid accumulation, consistent with the proposed model [64, 65]. Conversely, cessation of growth and movement has been observed to be accompanied by a decrease in hyaluronic acid production [66, 67]. Furthermore, Kraemer and his colleagues have isolated CHO cell variants in which the strength of cell-substratum adhesion is inversely correlated with the capacity to synthesize hyaluronic acid [68–70]. One subline is resistant to detachment from the substratum and synthesizes little or no hyaluronic acid, as well as reduced amounts of other complex carbohydrates at the cell periphery [68, 69]. Conversely, an easily detached variant has three times more detectable label in surface hyaluronic acid than does the parent cell [69]. Furthermore, in the parent CHO cell, an anchorage-dependent Chinese hamster cell line, the synthesis and deposition of hyaluronic acid into cell surface material is stimulated by cell attachment to and growth on a solid substratum [70]. All of these results are consistent with the negative modulatory role of hyaluronic acid (and some proteoglycans) in physiologically mature footpads proposed in our model.

In this model, then, the differences in adhesive strength between nontransformed and transformed cells could be explained in two ways. One possibility is that the adhesion sites of transformed cells accumulate more hyaluronic acid, galactosaminoglycan, and monovalent heparan sulfate, or less fibronectin, than do the adhesion sites of nontransformed cells. This would lead to a greater degree of cytoskeletal depolymerization and greater ease of detachment of transformed cells. However, we found no such differences between SAM prepared from transformed and nontransformed cell lines.

The other possibility is a defect in cytoskeletal organization or attachment to the membrane [71, 72]. Immunofluorescence and electron micrographic studies suggest that the cytoskeleton is, indeed, less well organized in transformed cells than in nontransformed cells [73–75]. Thus the material in SAM that actually effects adhesion of the cell surface to the substrate might be expected to be conserved in both normal and transformed cells, since both cell types are adhesive. Such conservation was, in fact, observed.

We believe that our model provides a reasonable interpretation for the available experimental evidence on cell-substratum adhesion, but many points clearly remain to be established. In particular, we are examining the physical and biochemical interactions between fibronectin and the proteoglycans and glycosaminoglycans in SAM, and we are examining more closely the roles of cell-surface-bound and substratum-bound fibronectin in the structure and function of SAM. Such studies should clarify the actual relationships between the various macromolecular components of SAM and may pave the way for a detailed molecular description of the cell-substratum adhesion site.

ACKNOWLEDGMENTS

We thank Josefina Buniel, Sara Hitri, and Riva Ansbacher for technical assistance, Dr. Martha Cathcart and Dr. Robert Haas for data and discussions, and Dr. Judy Schollmeyer for supplying results prior to publication. Dr. Richard Robson generously supplied samples of porcine skeletal muscle and chicken gizzard α-actinins. This work was supported in part by American Cancer Society research grant BC-217, National Cancer Institute research grant CA13513, and National Institute of Arthritis Metabolic and Digestive Diseases research grant AM 25646. Dr. Lloyd A. Culp was a Career Development Awardee of the

National Cancer Institute (CA70709). Ben A. Murray and Barrett J. Rollins were supported by U.S. Public Health Service Training grants GM 07225 and GM 07250, respectively.

NOTE ADDED IN PROOF

We now have additional evidence for fibronectin:proteoglycan binding in adhesion sites by examining the ability of GAGs isolated from substrate-attached material to bind to CIG-Sepharose columns. Most of the heparan sulfate in SAM binds very well to CIG, whereas the unsulfated and sulfated chondroitins do not bind [J. Laterra and L. Culp, unpublished data]. This supports the conclusion that multivalent heparan proteoglycans are direct mediators of the adhesive bond (Fig. 12).

REFERENCES

1. Culp LA: Curr Topics Memb Transport 11:327, 1978.
2. Hynes RO: Biochim Biophys Acta 458:73, 1976.
3. Yamada KM, Olden K: Nature 275:179, 1978.
4. Grinnell F: Int Rev Cytol 53:65, 1978.
5. Engvall E, Ruoslahti E: Int J Cancer 20:1, 1977.
6. Ruoslahti E, Vuento M, Engvall E: Biochim Biophys Acta 534:210, 1978.
7. Stathakis NE, Mosesson MW: J Clin Invest 60:855, 1977.
8. Grinnell F, Hays DG: Exp Cell Res 116:275, 1978.
9. Culp LA, Black PH: Biochemistry 11:2161, 1972.
10. Rosen JJ, Culp LA: Exp Cell Res 107:139, 1977.
11. Culp LA: Biochemistry 15:4094, 1976.
12. Rollins BJ, Culp LA: Biochemistry 18:141, 1979.
13. Culp LA, Bensusan H: Nature 273:680, 1978.
14. Cathcart MK, Culp LA: Biochemistry 18:1167, 1979.
15. Culp LA, Rollins BJ, Buniel J, Hitri S: J Cell Biol 79:788, 1978.
16. Terry AH, Culp LA: Biochemistry 13:414, 1974.
17. Culp LA: Exp Cell Res 92:467, 1975.
18. Mapstone TB, Culp LA: J Cell Sci 20:479, 1976.
19. Culp LA, Terry AH, Buniel JF: Biochemistry 14:406, 1975.
20. Culp LA, Buniel JF, Rosen JJ: In Harmon RE (ed): "Cell Surface Carbodydrate Chemistry." New York: Academic Press, 1978, p 205.
21. Culp LA: J Supramol Struct 5:239, 1976.
22. Harris AK: Dev Biol 35:97, 1973.
23. Revel JP, Hoch P, Ho D: Exp Cell Res 84:207, 1974.
24. Revel JP, Wolken K: Exp Cell Res 78:1, 1973.
25. Badley RA, Lloyd CW, Woods A, Carruthers L, Allcock C, Rees DA: Exp Cell Res 117:231, 1978.
26. Whur P, Koppel H, Urquhart CM, Williams DC: J Cell Sci 24:265, 1977.
27. Vessey AR, Culp LA: Virology 86:556, 1978.
28. Suzuki A, Goll DE, Singh I, Allen RE, Robson RM, Stromer MH: J Biol Chem 251:6860, 1976.
29. Mooseker MA, Tilney LG: J Cell Biol 67:725, 1975.
30. Lazarides E: J Cell Biol 68:202, 1976.
31. Brown S, Levinson W, Spudich JA: J Supramol Struct 5:119, 1976.
32. Starger JM, Goldman RD: Proc Natl Acad Sci USA 74:2422, 1977.
33. Hynes RO, Destree AT: Cell 13:151, 1978.
34. O'Farrell PH: J Biol Chem 250:4007, 1975.
35. Hynes RO, Destree A: Proc Natl Acad Sci USA 74:2855, 1977.
36. Whalen RG, Butler-Browne GS, Gros F: Proc Natl Acad Sci USA 73:2018, 1976.
37. Garrels JI, Gibson W: Cell 9:793, 1976.
38. Kuusela P, Ruoslahti E, Engvall E, Vaheri A: Immunochemistry 13:639, 1976.
39. Axelsen NH, Krøll J, Weeke B (eds): Scand J Immunol 2 (Suppl 1), 1973.

40. Olden K, Yamada KM: Anal Biochem 78:483, 1977.
41. Mautner V, Hynes RO: J Cell Biol 75:743, 1978.
42. Hedman K, Vaheri A, Wartiovaara J: J Cell Biol 76:748, 1978.
43. Albrecht-Buehler G: Cell 11:395, 1977.
44. Thom D, Powell AJ, Badley RA, Woods A, Smith CG, Rees DA: Ann NY Acad Sci 312:453, 1978.
45. Kraemer PM: Biochem Biophys Res Commun 78:1334, 1977.
46. Klebe RJ: Nature 250:248, 1974.
47. Pearlstein E: Nature 262:497, 1976.
48. Hynes RO, Destree AT, Mautner VM, Ali IU: J Supramol Struct 7:397, 1977.
49. Vaheri A, Kurkinen M, Lehto V-P, Linder E, Timpl R: Proc Natl Acad Sci USA 75:4944, 1978.
50. Pessac B, Defendi V: Science 175:898, 1972.
51. Underhill C, Dorfman A: Exp Cell Res 117:155, 1978.
52. Roblin R, Albert SO, Gelb NA, Black PH: Biochemistry 14:347, 1975.
53. Gail MH, Boone CW: Exp Cell Res 70:33, 1972.
54. Hardingham TE, Muir HE: Biochim Biophys Acta 279:401, 1972.
55. Hascall VC, Heinegård D: J Biol Chem 249:4232, 1974.
56. Hascall VC: J Supramol Struct 7:101, 1977.
57. Lindahl U, Höök M: Ann Rev Biochem 47:385, 1978.
58. Sajdera SW, Hascall VC: J Biol Chem 244:77, 1969.
59. Hascall VC, Sajdera SW: J Biol Chem 244:2384, 1969.
60. Horner AA: J Biol Chem 246:231, 1971.
61. Yurt RW, Leid RW Jr, Austen KF, Silbert JE: J Biol Chem 252:518, 1977.
62. Kleinman HK, McGoodwin EB, Klebe RJ: Biochem Biophys Res Commun 72:426, 1976.
63. Chen W-T: J Cell Biol 75:416a, 1977.
64. Tomida M, Koyama H, Ono T: J Cell Physiol 86:121, 1975.
65. Lembach KJ: J Cell Physiol 89:277, 1976.
66. Morris CC: Ann NY Acad Sci 86:179, 1960.
67. Tomida M, Koyama H, Ono T: Biochim Biophys Acta 338:352, 1974.
68. Atherly AG, Barnhart BJ, Kraemer PM: J Cell Physiol 90:375, 1977.
69. Barnhart BJ, Cox SH, Kraemer PM: (in preparation).
70. Kraemer PM, Barnhart BJ: Exp Cell Res 114:153, 1978.
71. Rees DA, Lloyd CW, Thom D: Nature 267:124, 1977.
72. Edelman GM: Science 192:218, 1976.
73. Willingham MC, Yamada KM, Yamada SS, Pouysségur J, Pastan I: Cell 10:375, 1977.
74. McNutt NS, Culp LA, Black PH: J Cell Biol 50:691, 1971.
75. McNutt NS, Culp LA, Black PH: J Cell Biol 56:412, 1973.